

KINETIC AND STRUCTURAL STUDY OF INTERFACIAL AGGREGATION OF MICROPARTICLES AT LIQUID-AIR INTERFACES

A. VINCZE, R. FATA, GY. PARLAGH, M. ZRÍNYI,
J. KERÉSZ and Z. HÓRVÖLCEVI

Abstract

Aggregation of glass spheres ($75 \pm 5 \mu\text{m}$ diameter) having different — medium and high — hydrophobicities was investigated at liquid-air interfaces (water-air, aqueous surfactant solution-air and aqueous glycerol solution-air) from morphological and kinetic point of view. The physical parameters of aggregation were calculated by computerized image analysis. The cluster structures were characterized by the fractal dimension calculated from the scaling law between radius of gyration and surface coverage of aggregates (growth function). The primary growth in every investigated case was accompanied by restructuring which makes the clusters denser and more compact. The kinetic order of aggregation was analyzed in terms of determining the number of clusters as a function of aggregation time. In the early stage of the aggregation the kinetics was second order in every investigated case but beyond a given time (and cluster size) the kinetics changed in the most cases.

1. Introduction

The studies of colloid aggregation at liquid-air interfaces attracted significant attention in the last decades [1-12]. In recent years the interfacial aggregation of spherical microparticles under the control of short-range colloid forces and long-range capillary forces was investigated intensively [13-18]. The aim of this work is to investigate how the morphology of clusters and the aggregation kinetics are influenced by the surface properties of particles (hydrophobicity) and by the composition of liquids used for the experiments (effect of viscosity and the surface tension).

2. Experimental part

2.1. Materials

Distilled water, aqueous glycerol solution (87%, Reanal, A. R.), aqueous surfactant solution (NaDS-Sodium dodecyl sulfate-, Reanal, purum, concentration:

0.06 $\frac{\text{mol}}{\text{dm}^3}$), and glass microbeads (Supelco, $75 \pm 5 \mu\text{m}$ diameter) were used for the aggregation experiments. The glycerol solution for the aggregation experiments was obtained by the dilution of the original glycerol by water: 2 vol. water + 1 vol. original glycerol solution. The surface of the glass beads was rendered hydrophobic by silylation [19]. The hydrophobicity was characterized by water contact angles (Θ) which were determined by a microscopic method [19]. Changing the extent of silylation, samples of a lower ($\Theta_1=68^\circ$) and of a higher ($\Theta_2=85^\circ$) hydrophobicity were prepared.

2.2. Methods

The aggregation experiments were carried out in Petri dishes. The glass particles were scattered uniformly onto the liquid surface. Due to the capillary forces and the temperature inhomogeneity in the boundary layer the particles began to aggregate. The surface concentration of glass beads was about 260 $\frac{\text{pieces}}{\text{cm}^2}$ in every case.

The aggregation phenomena were recorded by a black-and-white video camera and a video recorder. The recorded images were analyzed by a digitized image analyzing system. We developed a computer software for the determination of the characterizing parameters of clusters.

3. Physical quantities

The fractal dimension (D), the radius of gyration (R_g) and the surface coverage (q) were used to characterize the morphology of aggregates. The size of the cluster was characterized by the radius of gyration which is the trace of an inertia tensor [20]. Using this parameter, the surface coverage of an aggregate was approximated as follows:

$$(1) \quad q = \frac{M}{R_g^2 \pi}$$

where M is the total area covered by the particles of a cluster. Fractal dimension was determined for the series of the different sized clusters according to the scaling law between R_g and q :

$$(2) \quad q \propto R_g^{D-2}$$

The $\ln q$ vs. $\ln R_g$ graph is called the growth function. The geometry of an individual cluster was also characterized by the fractal dimension obtained by the Sand-box method [21].

The kinetic order of aggregation was studied by determining the number of clusters as a function of aggregation time [22]. If the aggregation kinetics is second order the aggregation rate can be derived from the following equation:

$$(3) \quad -\frac{dn}{dt} = kn^2$$

where n is the number of particles in a unit area at time, t and k is the rate constant. Integrating the equation (3) with $t=0$ and $n=n_0$:

$$(4) \quad \frac{1}{n} - \frac{1}{n_0} = kt$$

where n_0 is the initial number of kinetic units.

4. Experimental results and discussion

4.1. Visual observations and fractal dimensions for the individual final clusters

The characterizing images and their fractal dimensions of final aggregates for the investigated systems are given in Fig. 1.

As can be seen the clusters formed at aqueous surfactant solution-air interfaces are compact and their fractal dimension is around 2.0. The clusters formed by the less hydrophobic particles has higher fractal dimension than the clusters composed of more hydrophobic particles at water-air interface. The fractal dimensions for the higher and the lower hydrophobic samples were similar to each other at aqueous glycerol solution-air interface.

The reason for different morphology is the occurrence of restructuring within the clusters, which was observed visually. Restructuring which is attributed to the long-range capillary attraction forces [16, 18] means that particles after sticking can roll on each other forming closed loops and more compact clusters. The effect of restructuring on the cluster geometry is especially significant in case of the clusters composed of less hydrophobic particles because the short-range colloid attraction forces between particles are weaker, hence they are not able to prevent the clusters from restructuring [16, 18].

4.2. Growth functions and fractal dimensions for the series of different sized clusters

Two growth function types were observed (see Fig. 2a,b). The growth showed "cross-over" for both the lower and the higher hydrophobic samples at the water-air and at the aqueous glycerol solution-air interfaces (Fig. 2a). The first part of







Interface	$\Theta_1 = 68^\circ$	$\Theta_2 = 85^\circ$
Distilled Water - air	 $D = 1.84$	 $D = 1.73$
Aqueous surfactant solution - air	 $D = 2.00$	 $D = 2.00$
Aqueous glycerol solution - air	 $D = 1.88$	 $D = 1.86$
$N = 8000-10000$		

Fig. 1. The images of final aggregates of the investigated systems. D is the fractal dimension, N is the total number of particles

these graphs revealed fractal growth. During the second part of the growth, clusters lost their fractal morphology, became more compact because of the restructuring of clusters which was in good agreement with the visual observations. The second type of growth functions obtained at aqueous surfactant solution-air interfaces did not revealed neither fractal growth nor "cross-over". Compact clusters formed during the whole aggregation (Fig. 2b).

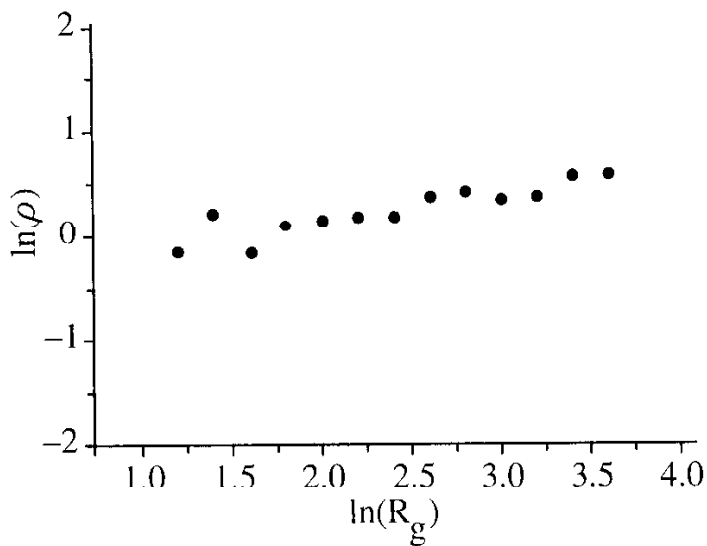
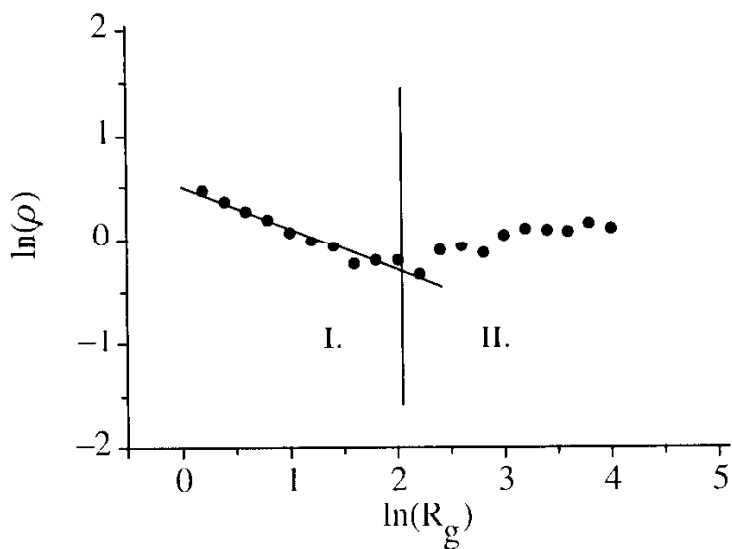


Fig. 2. Growth function of the lower hydrophobic glass beads at water-air interface (a) and at aqueous surfactant solution-air interface (b)

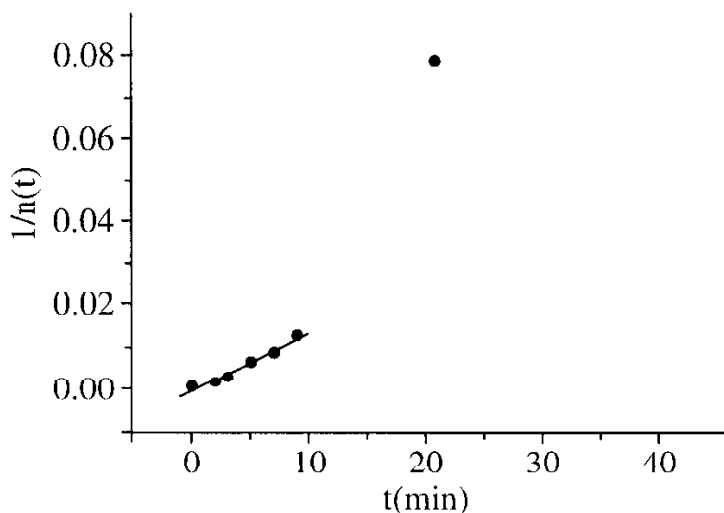
Interface	D($\Theta_1 = 68^\circ$)	D($\Theta_2 = 85^\circ$)
Water-air	1.60	1.50
Aqueous surfactant solution-air	non-fractal	non-fractal
Aqueous glycerol solution-air	1.37	1.38

Table 1.
Fractal dimensions calculated from the growth functions

The fractal dimensions calculated from the first part of the growth functions using the scaling law (2) can be seen in Table 1.

4.3. Kinetics

Fig. 3 shows $\frac{1}{n}$ vs. t graphs for the cases of less hydrophobic sample at different interfaces. The aggregation kinetics was found to be second order at aqueous surfactant solution-air (Fig. 3b) interface which is in a good agreement with the former results of three dimensional investigations [23] and with the Smoluchowsky concept about the colloid aggregations. In case of water-air and aqueous glycerol solution-air interfaces, the early stage of aggregation seemed to be second order, but at the final part of aggregation the kinetics changed (Fig. 3a,c).



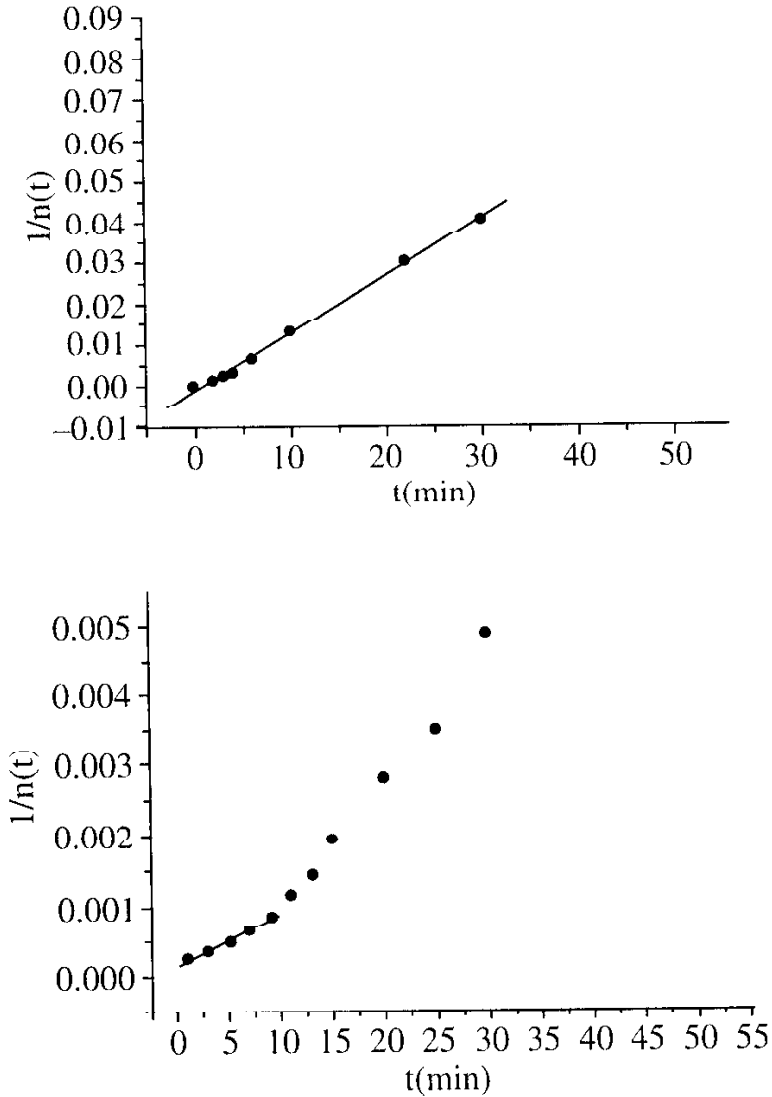


Fig. 3. $\frac{1}{n}$ vs. t graphs for the lower hydrophobic sample at water-air (a), aqueous surfactant solution-air (b) and aqueous glycerol solution-air (c) interfaces. The solid lines shows the linear part of the curves

The slopes of the fitted lines in Fig. 3 supply the aggregation rate constants which demonstrate the driving force of aggregation. Hence, the deviations from the fitted lines in Fig. 3a,c show an increase in the driving force with the aggregation time. The increasing driving force during the aggregation can be attributed to the increasing size of clusters. They cover a significant part of the liquid-air surface with the aggregation time, hence, their ability to capture a small cluster or particle increase. As expected, the growth rate of driving force is the most considerable in case of the water-air interface. The growth rate of cluster sizes at water-air interfaces is the most significant due to the relatively low liquid viscosity and the attractive colloid forces which partly hindered restructuring. On the other hand, increasing cluster size may result in more significant capillary attraction which also can lead to the growth of driving force of aggregation. These findings are in a total agreement with the results of the previous sections concerning the evaluations of cluster morphology at different interfaces.

ACKNOWLEDGEMENT. Support of this work by grants from OTKA (T023080 to Z. H. and T015754 to M. Z.) is gratefully acknowledged.

REFERENCES

- [1] C. ALLAIN and B. JOUIHER, *J. Phys. (Paris), Lett.* **44** (1983), 1-421.
- [2] A. J. HURD and D. W. SCHAEFER, *Phys. Rev. Lett.* **54** (1985), 1043.
- [3] A. T. SKJELTORP, *Phys. Rev. Lett.* **58** (1987), 1444.
- [4] A. T. SKJELTORP and G. HELGESEN, *NATO ASI Ser., Ser. E* **157** (Random Fluctuations Pattern Growth) (1988), 56-61.
- [5] J.-F. ROUSSEL, C. CAMOIN and R. BLANC, *J. Phys. (Paris)* **50** (1989), 3259.
- [6] J.-F. ROUSSEL, C. CAMOIN and R. BLANC, *J. Phys. (Paris)* **50** (1989), 3269.
- [7] D. J. ROBINSON and J. C. EARNSHAW, *Phys. Rev. A* **46** (4) (1992), 2045.
- [8] D. J. ROBINSON and J. C. EARNSHAW, *Phys. Rev. A* **46** (4) (1992), 2055.
- [9] D. J. ROBINSON and J. C. EARNSHAW, *Phys. Rev. A* **46** (4) (1992), 2065.
- [10] D. F. WILLIAMS and J. C. BERG, *J. Colloid Interface Sci.* **152** (1) (1992), 218-229.
- [11] P. A. KRALCHEVSKY and K. NAGAYAMA, *Langmuir* **10** (1994), 23.
- [12] D. J. ROBINSON and J. C. EARNSHAW, *Langmuir* **9** (1993), 1436.
- [13] Z. HÓRVÖLGYI, M. MEDVECZKY and M. ZRÍNYI, *Colloids Surfaces* **60** (1991), 79-95.

- [14] Z. HÓRVÖLGYI, M. MEDVECZKY and M. ZRÍNYI, *Colloid Polymer Sci.* **271** (1993), 396-403.
- [15] Z. HÓRVÖLGYI and M. ZRÍNYI, *Fractals* **1** (3) (1993), 460-469.
- [16] Z. HÓRVÖLGYI, M. MÁTÉ and M. ZRÍNYI, *Colloids Surfaces A: Physicochemical Asp.* **84** (1994), 207-216.
- [17] M. MÁTÉ, M. ZRÍNYI and Z. HÓRVÖLGYI, *Colloids Surfaces A: Physicochemical Asp.* **108** (1996), 147-157.
- [18] A. VINCZE, R. FATA, M. ZRÍNYI, Z. HÓRVÖLGYI and J. KERTÉSZ, *J. Chem. Phys.* **107** (18) (1997), 7451.
- [19] Z. HÓRVÖLGYI, S. NÉMETH and J. H. FENDLER, *Langmuir* **12** (4) (1996), 997-1004.
- [20] FAMILY, T. VICSEK and P. MEAKIN, *Phys. Rev Lett.* **55** (1985), 641.
- [21] T. VICSEK, *Fractal Growth Phenomena* (Second edition), World Scientific, Singapore, 1992, 13-14.
- [22] D. J. SHAW, *Bevezetés a kolloid- és felületi kémiába*, Műszaki Könyvkiadó, Budapest, 1986.
- [23] H. SONNTAG and K. STRENGE, *Coagulation kinetics and structure formation*, Plenum Press, New York, 1987.

A. VINCZE, R. FATA, GY. PARLAGH, M. ZRÍNYI, Z. HÓRVÖLGYI
DEPARTMENT OF PHYSICAL CHEMISTRY TECHNICAL UNIVERSITY OF BUDAPEST
H-1521 BUDAPEST
HUNGARY

J. KERTÉSZ
DEPARTMENT OF THEORETICAL PHYSICS
TECHNICAL UNIVERSITY OF BUDAPEST
H-1521 BUDAPEST
HUNGARY